THE JOURNAL OF BIOLOGICAL CHEMISTRY VOL. 290, NO. 18, pp. 11663–11677, May 1, 2015

Opposite Cross-Talk by Oleate and Palmitate on Insulin Signaling in Hepatocytes through Macrophage Activation*

Received for publication, March 3, 2015 Published, JBC Papers in Press, March 19, 2015, DOI 10.1074/jbc.M115.649483

Virginia Pardo[‡§], **Águeda González-Rodríguez**[‡§1], **Carlos Guijas**[§¶], **Jesús Balsinde**[§¶], **and Ángela M. Valverde**[§¶2]

From the [‡]*Instituto de Investigaciones Biomédicas Alberto Sols (Consejo Superior de Investigaciones Científicas/Universidad Autónoma de Madrid), 28029 Madrid, Spain, the* [§]*Centro de Investigación Biomédica en Red de Diabetes y Enfermedades Metabólicas Asociadas (CIBERDEM), Instituto de Salud Carlos III, 28029 Madrid, Spain, and the* [¶]*Instituto de Biología y Genética Molecular (Consejo Superior de Investigaciones Científicas), 47003 Valladolid, Spain*

Background: Chronic low grade inflammation during obesity is associated with impairments in the insulin signaling cascade.
Results: Oleate and palmitate elicit opposite effects in insulin signaling in hepatocytes through macrophage stimulation.
Conclusion: An endocrine/paracrine cross-talk between macrophages/Kupffer cells and hepatocytes modulates insulin signaling.
Significance: Switching macrophage/Kupffer cell polarization will be of benefit against insulin resistance in the liver.

Chronic low grade inflammation in adipose tissue during obesity is associated with an impairment of the insulin signaling cascade. In this study, we have evaluated the impact of palmitate or oleate overload of macrophage/Kupffer cells in triggering stress-mediated signaling pathways, in lipoapoptosis, and in the cross-talk with insulin signaling in hepatocytes. RAW 264.7 macrophages or Kupffer cells were stimulated with oleate or palmitate, and levels of M1/M2 polarization markers and the lipidomic profile of eicosanoids were analyzed. Whereas proinflammatory cytokines and total eicosanoids were elevated in macrophages/Kupffer cells stimulated with palmitate, enhanced arginase 1 and lower leukotriene B_4 (LTB_4) levels were detected in macrophages stimulated with oleate. When hepatocytes were pretreated with conditioned medium (CM) from RAW 264.7 or Kupffer cells loaded with palmitate (CM-P), phosphorylation of stress kinases and endoplasmic reticulum stress signaling was increased, insulin signaling was impaired, and lipoapoptosis was detected. Conversely, enhanced insulin receptor-mediated signaling and reduced levels of the phosphatases protein tyrosine phosphatase 1B (PTP1B) and phosphatase and tensin homolog (PTEN) were found in hepatocytes treated with CM from macrophages stimulated with oleate (CM-O). Supplementation of CM-O with LTB_4 suppressed insulin sensitization and increased PTP1B and PTEN. Furthermore, LTB_4 decreased insulin receptor tyrosine phosphorylation in hepatocytes, activated the NFκB pathway, and up-regulated PTP1B and PTEN, these effects being mediated by LTB_4 receptor BTL1. In conclusion, oleate and palmitate elicit an opposite cross-talk between macrophages/Kupffer cells and hepatocytes. Whereas CM-P interferes at the early steps of insulin signaling, CM-O increases insulin sensitization, possibly by reducing LTB_4.

Evidence from clinical and epidemiological studies has clearly established that obesity is the most common cause of insulin resistance, type 2 diabetes mellitus and non-alcoholic fatty liver disease. In fact, insulin resistance in peripheral tissues, such as liver and skeletal muscle, is an early metabolic abnormality in the development of type 2 diabetes mellitus (1). Although the precise molecular mechanisms underlying insulin resistance associated with obesity have not been completely elucidated, one major contributor is the chronic low grade systemic inflammation state that interferes with the early steps of the insulin signaling cascade, possibly through the effects of free fatty acids (FFAs)[3] and cytokines secreted by the overgrowing white adipose tissue (2–4).

Proinflammatory cytokines impair insulin action by activating stress kinases such as c-Jun NH_2-terminal kinase (JNK), IκB kinase (IKK), and also protein kinase C (PKC)-mediated pathways (5, 6). In addition, cytokines down-regulate early key mediators of the insulin signaling cascade, such as the insulin receptor (IR) or insulin receptor substrate 1 (IRS1) (7, 8), as well as increase the expression of negative modulators of this pathway, such as the protein-tyrosine phosphatase 1B (PTP1B) (9, 10). On the other hand, circulating FFAs, which are usually increased in insulin-resistant states (11–13), also activate these

* This work was supported by Ministerio de Economía y Competitividad, Spain, Grants SAF2012-33283 and SAF2013-48201-R; Comunidad de Madrid Grant S2010/BMD-2423 (Spain); an European Foundation for the Studies of Diabetes and Amylin Paul Langerhans grant; and the Centro de Investigación Biomédica en Red de Diabetes y Enfermedades Metabólicas Asociadas (CIBERDEM, Instituto de Salud Carlos III, Spain).
[1] Holder of a CIBERDEM (ISCIII) postdoctoral contract. To whom correspondence may be addressed: Instituto de Investigaciones Biomédicas Alberto Sols, C/ Arturo Duperier 4, 28029 Madrid, Spain. Tel.: 34-915854497; Fax: 34-915854401; E-mail: aguedagr@iib.uam.es.
[2] To whom correspondence may be addressed: Instituto de Investigaciones Biomédicas Alberto Sols, C/ Arturo Duperier 4, 28029 Madrid, Spain. Tel.: 34-915854497; Fax: 34-915854401; E-mail: avalverde@iib.uam.es.

[3] The abbreviations used are: FFA, free fatty acid; PTP1B, protein tyrosine phosphatase 1B; PTEN, phosphatase and tensin homolog; IR, insulin receptor; IRS, insulin receptor substrate; CM, conditioned medium/media; CM-P, CM-O, or CM-B, CM treated with palmitate, oleate, or BSA, respectively; IKK, IκB kinase; ER, endoplasmic reticulum; PG, prostaglandin; LT, leukotriene; CHOP, transcription factor C/EBP homologous protein; 11-HETE, 11-hydroxy-5Z,8Z,12E,14Z-eicosatetraenoic acid; 12-HHT, 12S-hydroxy-5Z,8E,10E-heptadecatrienoic acid; 15-HETE, 15-hydroxy-5Z,8Z,11Z,13E-eicosatetraenoic acid.

proinflammatory pathways, boosting the defects in peripheral insulin actions (14–16).

In addition to the inflammatory effects, the activation of endoplasmic reticulum (ER) stress-mediated signaling pathways by FFAs has been linked to obesity-associated immunometabolic dysregulation and insulin resistance (17, 18). ER stress is sensed by three main proteins, X-BP1 (X-box-binding protein 1), PERK (PRKR-like endoplasmic reticulum kinase), and ATF6 (activating transcription factor-6), which cooperate to mitigate ER stress by reducing protein translation, stabilizing proteins by chaperones, and activating ER-associated protein degradation (19). Chemical chaperones (tauroursodeoxycholic acid and 4-phenylbutryate) that alleviate ER stress through protein stabilization, improve systemic glucose homeostasis, increase glucose uptake in adipose and skeletal muscle, and reduce hepatic glucose production (20). Moreover, a study in obese subjects has revealed that treatment with tauroursodeoxycholic acid increases insulin sensitivity in liver and skeletal muscle by ~30% compared with the placebo therapy (21).

FFA-derived metabolites are relevant factors in the pathogenesis of the metabolic syndrome (22). Eicosanoids (prostaglandins (PGs), tromboxanes, leukotrienes (LTs), and cytochrome P450 metabolites) are bioactive lipids synthesized from polyunsaturated FFAs, such as proinflammatory ω-6 arachidonic acid or anti-inflammatory ω-3 eicosapentaenoic acid, and docosahexaenoic acid through the cyclooxygenases, lipoxygenases, and cytochrome P450 pathways. The functional role of eicosanoids in obesity and insulin resistance has recently been studied in humans and animal models. For instance, an accumulation of polyunsaturated FFAs, leukotriene B4 (LTB_4), and 6-keto-prostaglandin-$F_{1\alpha}$ was observed in plasma from patients with metabolic syndrome (23). Moreover, the development of insulin resistance in patients affected by metabolic syndrome leads to increased synthesis of thromboxane A_2. Regarding studies in cellular and animal models, it was shown that PGE_2 aggravates insulin resistance induced by interleukin 6 (IL6) in hepatocytes (24), whereas BLT1 (LTB_4 receptor 1)-deficient mice are resistant to high fat diet-induced obesity and insulin resistance (25).

Several studies have reported that besides adipocytes, adipose tissue resident macrophages, which migrate and accumulate in white adipose tissue, have a relevant role in obesity-induced chronic inflammation (26–28) through their polarization toward the M1-like state (29). Although the importance of macrophages in the molecular mechanisms triggering insulin resistance in skeletal muscle and adipose tissue has been explored (29–31), it remains unclear whether the inflammatory milieu impacts insulin signaling in hepatocytes. On that basis, in this study, we have investigated for the first time the effect of macrophages activated by two distinct FFAs, palmitate (saturated) and oleate (unsaturated), on stress-mediated pathways, lipoapoptosis, and the insulin signaling cascade in hepatocytes.

EXPERIMENTAL PROCEDURES

Reagents—Fetal bovine serum (FBS) (catalog no. 10270) and culture medium DMEM (catalog no. 41966–029) were obtained from Invitrogen. TRIzol reagent (catalog no. T9424), sodium palmitate (catalog no. P9767), sodium oleate (catalog no. O7501), bovine serum albumin (BSA) (catalog no. A6003), fatty acid-free BSA endotoxin-free (catalog no. A8806), and insulin (catalog no. I0516) were from Sigma-Aldrich. Bradford reagent, acrylamide, immunoblotting PVDF membrane, and Immobilon Western chemiluminescent HRP substrate were purchased from Bio-Rad.

Free Fatty Acid Preparation—2.5 mM FFA stock solutions were prepared by a modification of the Spector method (32). Briefly, cold sodium palmitate or sodium oleate was dissolved in 0.1 M NaOH by heating at 70 °C while 0.5 mM BSA solution was prepared by dissolving fatty acid-free BSA in NaCl 0.9% by heating at 50 °C (at maximum). Once BSA and FFA solutions were completely dissolved, palmitate and oleate solutions were diluted 10 times in the BSA solution and mixed by pipetting to achieve a final molar ratio of 5:1. Control BSA was prepared by adding the same amount of 0.1 M NaOH into 0.5 mM BSA solution. All preparations were filtered, aliquoted, and stored at −20 °C.

Culture of RAW 264.7 Murine Macrophages and Immortalized Hepatocytes—The murine RAW 264.7 macrophage cell line, kindly provided by Dr. Tarín (CNIC, Madrid, Spain), was cultured in RPMI supplemented with 10% heat-inactivated FBS, 100 units/ml penicillin, 100 μg/ml streptomycin, and 2 mM glutamine. The generation and characterization of immortalized mouse hepatocyte cell line have been described previously (33). Cells were grown in DMEM plus 10% heat-inactivated FBS, 100 units/ml penicillin, 100 μg/ml streptomycin, and 2 mM glutamine. Confluent macrophages were treated with BSA or FFA solutions (750 μM conjugated oleate/BSA or 750 μM conjugated palmitate/BSA) for 24 h to obtain the corresponding conditioned medium (CM) (31). CM were centrifuged to remove dead cells and directly added (without dilution) to hepatocytes for several time periods. In all experiments, comparable mRNA levels of pro- and anti-inflammatory markers were observed in RAW 264.7 macrophages.

Isolation and Culture of Kupffer Cells—For Kupffer cell isolation, the supernatant from the first centrifugation of the hepatocyte isolation protocol was collected and centrifuged twice at 50 × *g* for 5 min to discard the pellet with the remaining hepatocytes. The latest supernatant was centrifuged at 500 × *g* for 5 min at 4 °C, and the pellet containing the Kupffer cells was resuspended in attachment medium. Cells were mixed by inversion with 50% Percoll and centrifuged at 1.059 × *g* for 30 min without acceleration or brake at room temperature. Finally, the Kupffer cell pellet was washed with 1× PBS and centrifuged twice at 500 × *g* for 10 min at 4 °C to wash out the residual Percoll solution, and cells were resuspended in RPMI supplemented with 10% heat-inactivated FBS, 100 units/ml penicillin, 100 μg/ml streptomycin, and 2 mM glutamine. Cells were then plated on 12-well plates and maintained for 24 h before treatments. Conditioned medium was prepared as described in RAW 264.7 cells.

Primary Hepatocyte Cell Culture—Human hepatocytes were isolated by the two-step collagenase procedure from non-tumor areas of liver biopsies from patients submitted to a surgical resection for liver tumors after obtaining patients' written consent (34). Primary mouse hepatocytes were isolated from non-

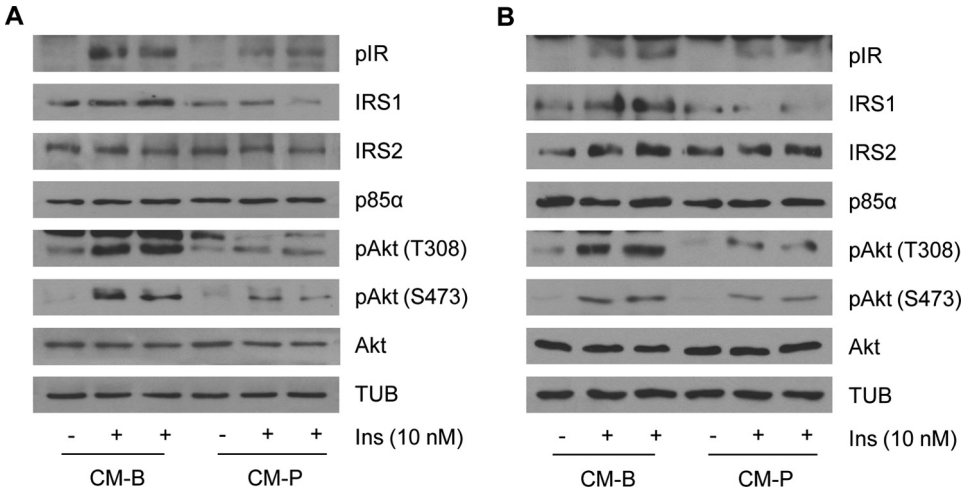

FIGURE 1. **Proinflammatory components of the conditioned medium from RAW 264.7 macrophages stimulated with palmitate are mediators of the impairment in insulin signaling in hepatocytes.** Hepatocytes were treated 24 h with conditioned media collected from RAW 264.7 cells treated with BSA (*CM-B*) or palmitate (*CM-P*) for 24 h (*A*) or with conditioned media collected from RAW 264.7 cells treated with BSA (*CM-B*) or palmitate (*CM-P*) for 8 h and then reefed with fresh medium for a further 16 h (*B*). Then cells were stimulated with 10 nM insulin for 10 min. Total protein was analyzed by Western blot using the indicated antibodies. Representative blots are shown ($n = 3$ experiments performed in duplicate).

fasting male C57BL/6 mice (10–12 weeks old) by perfusion with collagenase as described (35). Cells were seeded on a 6-well plate (Corning, Inc.) and cultured in medium containing Dulbecco's modified Eagle's medium and Ham's F-12 medium (1:1) with 10% FBS, supplemented with 2 mM glutamine, 100 units/ml penicillin, 100 μg/ml streptomycin, and 1 mM sodium pyruvate (attachment medium) and maintained for 24 h before treatments. The generation and characterization of the immortalized mouse hepatocyte cell line have been described previously (33).

Transfection with siRNA—siRNA oligonucleotides were synthesized by Ambion (Life Technologies) for gene silencing of mouse BLT1 and arginase 1. Immortalized mouse hepatocytes or RAW 264.7 macrophages were seeded in 6-cm dishes and incubated at 37 °C with 5% CO_2 overnight. When 40–50% confluence was reached, cells were transfected with BLT1 or arginase 1 siRNA at different concentrations (5–25 nM) or with a scrambled siRNA, used as a control. After 36 h, cells were used for experiments.

Analysis of FFA-derived Metabolites—0.01% (w/v) of butylated hydroxytoluene in methanol was added to supernatants to prevent metabolite degradation. CM collected from macrophages treated with BSA or FFAs solutions were melted slowly, and 400 pmol of deuterated PGE_2 and LTB_4 were added as internal standards before solid phase extraction. Lipid metabolites were extracted using Bond Elut Plexa solid phase extraction columns (Agilent Technologies, Santa Clara, CA) as indicated by the manufacturer. Columns were homogenized with 3 ml of methanol followed by 3 ml of water. Supernatants were acidified with 0.5% acetic acid, and 10% methanol was also added before sample loading. Samples were washed with 3 ml of 10% methanol, and finally, lipid products were eluted with 2 × 1.5 ml of 100% methanol. Lipid metabolites were concentrated under vacuum and redissolved in 100 μl of solvent A (water/acetonitrile/acetic acid, 70:30:0.02 (v/v/v)) for their analysis by HPLC/MS/MS. The chromatographic protocol was adapted from Dumlao *et al.* (36). Quantification was carried out by the integration of chromatographic peaks of the previously identified species compared with an external calibration curve made with analytical standards. The software Analyst 1.5.2 was employed in this process.

Preparation of Protein Extracts and Western Blot—To obtain total cell lysates, attached cells were scraped off and incubated for 10 min on ice with lysis buffer (25 mM HEPES, 2.5 nM EDTA, 0.1% Triton X-100, 1 mM PMSF, and 5 μg/ml leupeptin). After protein content determination with Bradford reagent, total protein was boiled in Laemmli sample buffer and submitted to 8–15% SDS-PAGE. Proteins were transferred to immunoblot PVDF membrane, and, after blocking with 3% BSA or 5% nonfat dry milk, membranes were incubated overnight with several antibodies, as indicated. Immunoreactive bands were visualized using the ECL Western blotting protocol. Densitometric analysis of the bands was performed using ImageJ software. The anti-phospho-PERK (Thr-980) (catalog no. 3179), anti-phospho-eIF2α (Ser-51) (catalog no. 9721), anti-phospho-JNK (catalog no. 9251), anti-phospho-STAT3 (catalog no. 9131), anti-phospho-MAPK (catalog no. 9101), and anti-MAPK (catalog no. 4695) antibodies were from Cell Signaling Technology (Danvers, MA). The anti-JNK (sc-571), anti-IR β (sc-711), anti-PERK (sc-13073), anti-eIF2α (sc-11386), anti-GRP78 (sc-376768), anti-CHOP (sc-7351), anti-phospho-p38 (sc-17852), anti-p38 (sc-9212), anti-IRS1 (sc-559), anti-IRS2 (sc-8299), anti-phospho-IR (sc-25103), anti-phospho-Akt (Thr-308) (sc-16646), anti-phospho-Akt (Ser-473) (sc-7985), anti-Akt (sc-8312), anti-PTP1B (sc-1718), and anti-PTEN (sc-7974) antibodies were from Santa Cruz Biotechnology, Inc. Anti-α-tubulin (T5168) and anti-β-actin antibodies (A5441) were from Sigma-Aldrich. Anti-arginase 1 antibody (610708) was purchased from BD Biosciences.

RNA Isolation and Quantitative PCR—Total RNA was isolated using TRIzol reagent and was reverse transcribed using a SuperScript™ III First-Strand Synthesis System for quantitative PCR following the manufacturer's indications. Quantitative PCR was performed with an ABI 7900 sequence detector

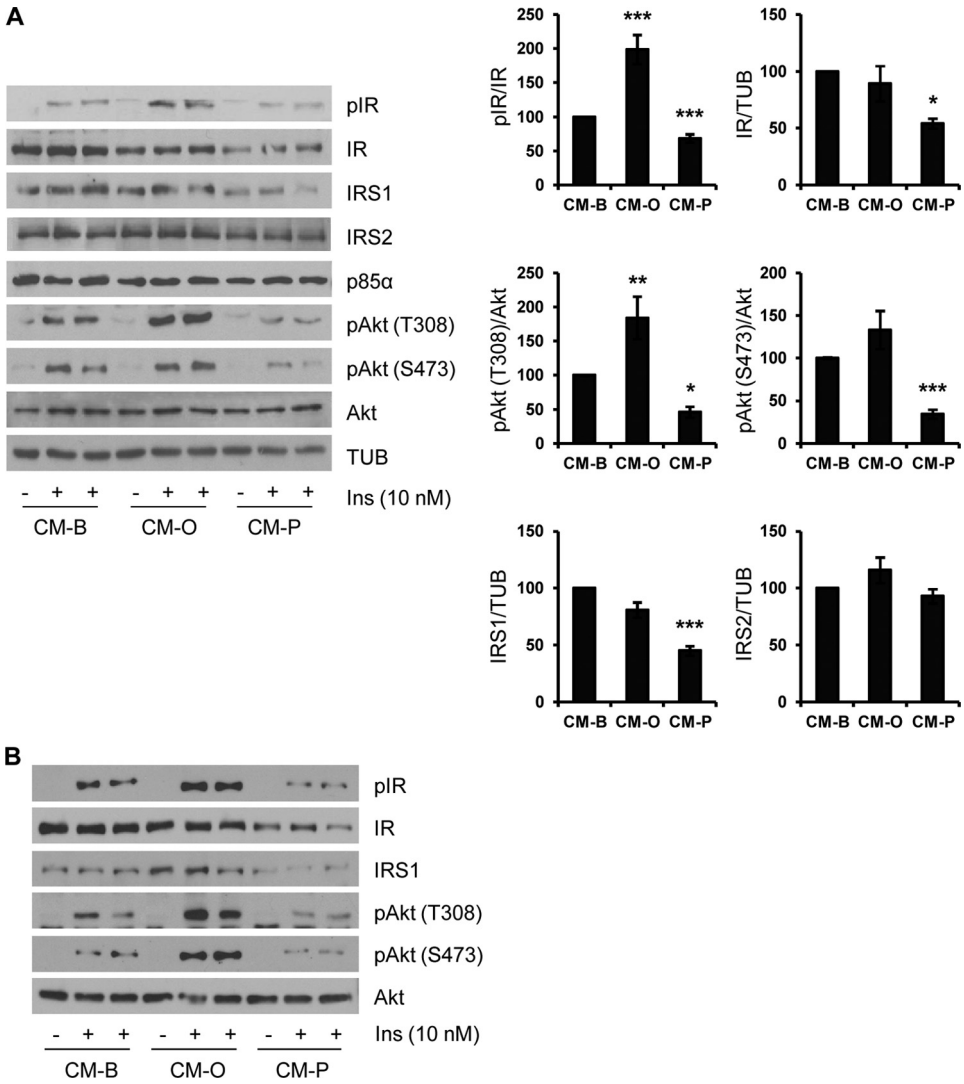

FIGURE 2. **Insulin signaling is differentially modulated in hepatocytes pretreated with conditioned medium from RAW 264.7 macrophages stimulated with oleate or palmitate.** *A*, conditioned medium from RAW 264.7 macrophages treated with BSA (*CM-B*), oleate (*CM-O*), or palmitate (*CM-P*) was added to immortalized mouse hepatocytes for 24 h. Then cells were stimulated with 10 nM insulin for 10 min. Total protein was analyzed by Western blot using the indicated antibodies. Representative blots are shown. After quantification of all blots, results are expressed as the percentage of insulin stimulation or percentage of protein expression relative to the CM-B condition (100%) and are mean ± S.E. (*error bars*) ($n = 6$ independent experiments performed in duplicate). *, $p < 0.05$; **, $p < 0.01$; ***, $p < 0.001$, CM-O or CM-P, respectively, *versus* CM-B. *B*, human primary hepatocytes were treated with conditioned medium from RAW 264.7 macrophages treated with BSA, oleate, or palmitate as described in *A*. Total protein was analyzed by Western blot using the indicated antibodies. Representative blots are shown ($n = 4$ experiments performed in duplicate).

using the SYBR Green method and d(N)6 random hexamer with primers purchased from Invitrogen. PCR thermocycling parameters were 95 °C for 10 min, 40 cycles of 95 °C for 15 s, and 60 °C for 1 min. Each sample was run in triplicate and normalized to 18 S RNA. -Fold changes were determined using the $\Delta\Delta Ct$ method. Primer sequences are available upon request.

Quantification of Apoptosis—Cells were grown in glass coverslips and treated as described above. Then cells were washed twice with PBS and fixed in *p*-formaldehyde (4%) for 10 min, and characteristic morphological changes of apoptosis were assessed by staining nuclei with DAPI followed by the analysis by fluorescence microscopy.

Statistical Analysis—Data are presented as mean ± S.E. and were compared by using the Bonferroni analysis of variance test. All statistical analyses were performed using IBM SPSS Statistics 21.0 (SPSS Inc., IBM, Armonk, NY) software with two-sided tests. Differences were considered statistically significant at $p < 0.05$.

RESULTS

Conditioned Medium from Macrophages Stimulated with Palmitate (CM-P) Impairs Insulin Signaling in Mouse Hepatocytes—The liver is composed primarily of hepatocytes but also contains blood and lymph vessels, nerves, and immune cells. Because all of these cell types can potentially respond to a high fat-mediated inflammatory environment *in vivo*, we used a cell culture-based approach to investigate the specific cross-talk between macrophages and hepatocytes in the context of fatty acid overload. For this goal, RAW 264.7 macrophages were treated with palmitate, a typical saturated FFA found in Western diets, for 24 h. Then, culture medium (conditioned

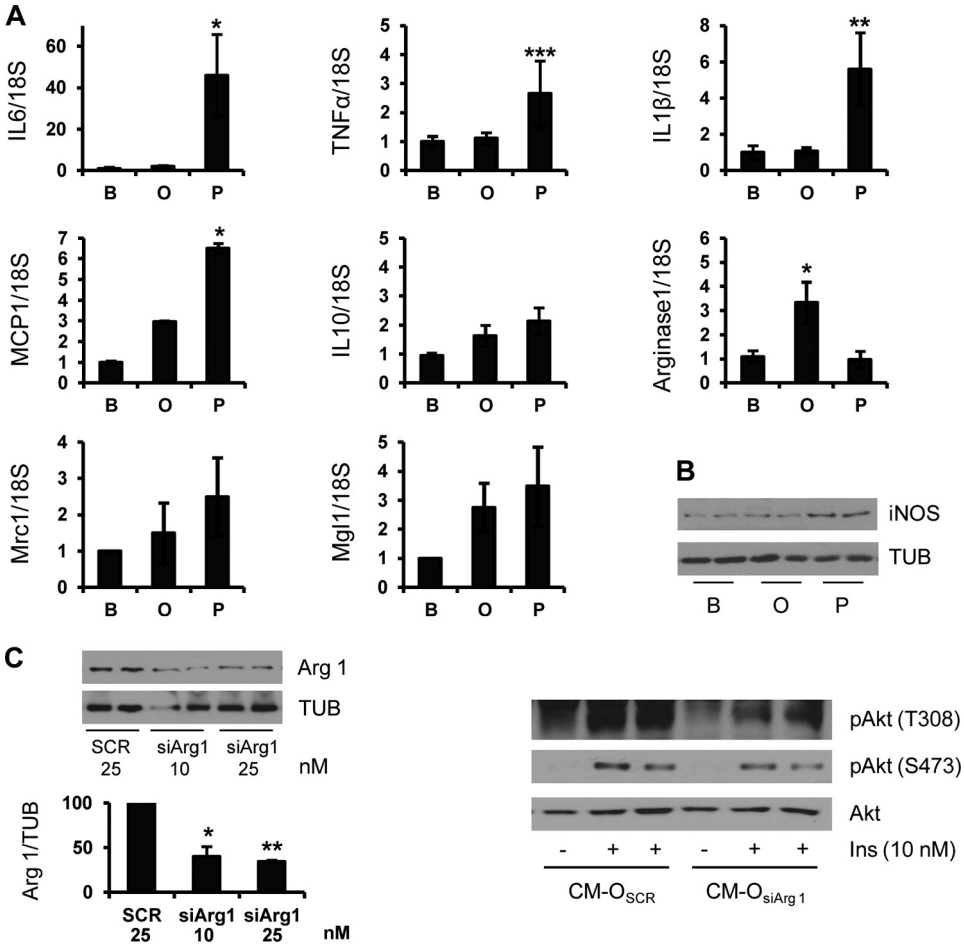

FIGURE 3. **Palmitate, but not oleate, treatment induces proinflammatory cytokine and chemokine gene expression in RAW 264.7 macrophages.** RAW 264.7 macrophages were treated with BSA (*B*), oleate (*O*), or palmitate (*P*) for 24 h. *A*, TNFα, IL-6, IL-1β, MCP1, IL-10, arginase 1, Mcr1, and Mgl1 mRNA levels were analyzed by quantitative RT-PCR. Results are expressed as -fold increase relative to the BSA condition and are mean ± S.E. (*error bars*) ($n \geq 4$). *, $p < 0.05$; **, $p < 0.01$; ***, $p < 0.001$, O or P, respectively, *versus* B. *B*, total protein was analyzed by Western blot using the indicated antibodies. Representative blots are shown ($n = 4$ experiments performed in duplicate). *C*, RAW 264.7 macrophages were transfected with arginase 1 or scrambled siRNA oligonucleotides, and after 36 h, oleate was added for a further 24 h. *Left*, protein levels of arginase 1 were analyzed by Western blot. Results are expressed as the percentage of decrease relative to the scrambled condition (100%) and are mean ± S.E. ($n = 3$ independent experiments performed in duplicate). *, $p < 0.05$; **, $p < 0.01$ arginase 1 siRNA *versus* scrambled. *Right*, CM of RAW 264.7 cells transfected with scrambled or arginase 1 siRNA (25 nM) and treated for 24 h with oleate (*CM-O$_{scr}$* or *CM-O$_{siArg1}$*, respectively) was added to mouse hepatocytes. After 24 h, hepatocytes were stimulated with 10 nM insulin for 10 min. Total protein was analyzed by Western blot using the indicated antibodies. Representative blots are shown ($n = 3$ independent experiments performed in duplicate).

medium) was removed. Conditioned medium was hereafter called CM-P (collected from RAW 264.7 cells treated with palmitate) or CM-B (from RAW 264.7 cells treated only with BSA as a control). CM-B or CM-P was added to immortalized mouse hepatocytes generated and validated in our laboratory (33) for a further 24 h, and then cells were stimulated with 10 nM insulin for 10 min. As depicted in Fig. 1*A*, IR tyrosine phosphorylation was reduced in hepatocytes preincubated with CM from palmitate-treated macrophages compared with those treated with control CM-B. Likewise, levels of IRS1 decreased only in hepatocytes treated with CM-P in parallel with decreases in Akt Ser-473 and Thr-308 phosphorylation in response to insulin. Notably, we found similar impairment of the insulin signaling in hepatocytes treated with CM collected from RAW 264.7 cells stimulated with palmitate for 8 h and then refed with fresh medium for a further 16 h (Fig. 1*B*). These results indicate that the components of the CM-P are sufficient to mediate the negative effects observed in insulin signaling in hepatocytes.

Insulin Signaling Is Oppositely Modulated in Mouse and Human Hepatocytes Pretreated with Conditioned Medium from Macrophages Stimulated with Palmitate or Oleate—Next, we checked that the effects of CM-P on insulin signaling in hepatocytes were specific to palmitate treatment and not due to the FFA overload. For this goal, we obtained conditioned medium from RAW 264.7 cells treated with oleate, a well known nontoxic monounsaturated FFA. Conditioned medium was hereafter called CM-O (collected from RAW 264.7 cells treated with oleate). After the addition of CM-B, CM-O, or CM-P for 24 h, immortalized mouse hepatocytes were stimulated with 10 nM insulin for 10 min. As depicted in Fig. 2*A*, insulin-induced IR tyrosine phosphorylation was enhanced in hepatocytes preincubated with CM-O as compared with control hepatocytes preincubated with control CM-B. As stated above (Fig. 1*A*), IR tyrosine and Akt phosphorylation was reduced in the presence of CM-P (Fig. 2*A*). Moreover, protein levels of IR and IRS1 decreased only in hepatocytes treated with CM-P. In agreement with enhanced IR tyrosine phosphoryla-

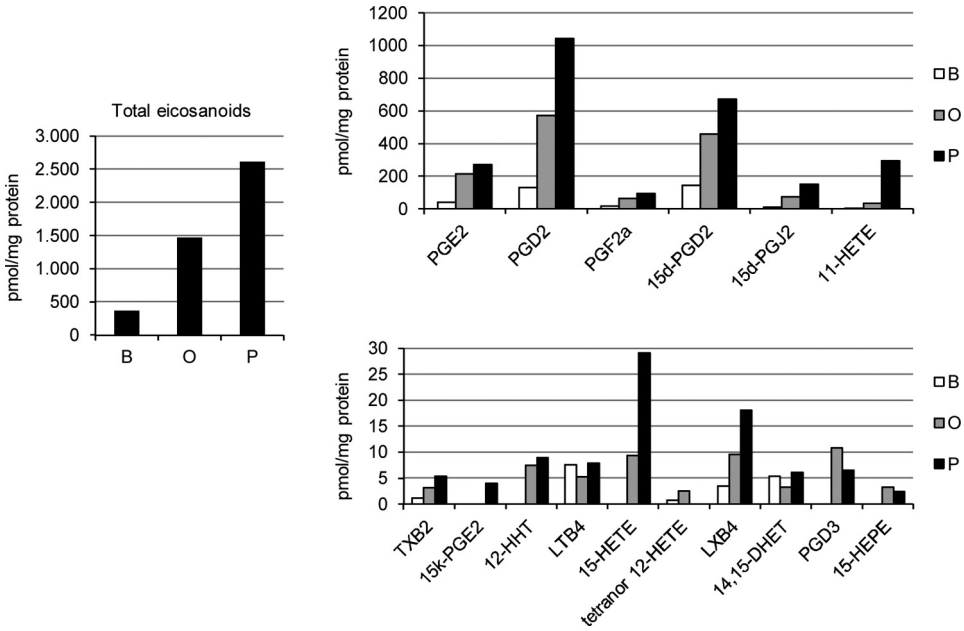

FIGURE 4. **Differential effect of palmitate and oleate in total eicosanoid content in RAW 264.7 macrophages.** Analysis of eicosanoids from the CM from RAW 264.7 macrophages treated with BSA (*B*), oleate (*O*), or palmitate (*P*) by high performance liquid chromatography/tandem mass spectrometry. Results are expressed as pmol/mg of protein. Data are shown as means of three independent experiments with triplicate determinations. In all cases, S.E. was below 10%; therefore, error bars were omitted for the sake of clarity.

tion and the maintenance of intact levels of IR and IRS1, the response to insulin in Akt phosphorylation at both residues was increased in hepatocytes treated with CM-O compared with those treated with CM-B. Notably, IRS2 levels were not affected by treatment of hepatocytes with either CM. Then the differential effect of both types of CM was assessed in human primary hepatocytes. Fig. 2*B* shows that the decreased IR/IRS1/Akt-mediated insulin signaling was also observed in human primary hepatocytes pretreated with CM-P, whereas a significant enhancement of this signaling pathway was found in human hepatocytes pretreated with CM-O. Altogether, these results indicate opposite effects of palmitate and oleate in triggering cross-talks between macrophages and hepatocytes with relevant effects in insulin signaling.

Differential Effects on the Content of Proinflammatory Cytokines and Eicosanoids Secreted by Macrophages Stimulated with Palmitate or Oleate—In an attempt to characterize the molecules released by macrophages to the CM, we assessed the expression of proinflammatory cytokines characteristic of M1 macrophage polarization by real-time PCR. Treatment of RAW 264.7 macrophages with palmitate, but not oleate, increased IL6, IL1β, TNFα, and MCP1 mRNA levels (Fig. 3*A*). Moreover, the induction of inducible nitric-oxide synthase, a key proinflammatory marker, was only detected in RAW 264.7 cells treated with palmitate (Fig. 3*B*). On the other hand, oleate treatment significantly up-regulated mRNA levels of arginase 1, a relevant M2 anti-inflammatory enzyme. Notably, no significant differences were observed in other M2 polarization markers, such as IL10, Mcr1, and Mgl1. The elevated levels of arginase 1 found in RAW 264.7 macrophages treated with oleate prompted us to further investigate its role in the cross-talk between macrophages and hepatocytes. For this goal, RAW 264.7 cells were transfected with control (scrambled) or arginase 1 siRNA. After 36 h, cells were treated with oleate for a further 24 h. CM-O of scrambled or arginase 1 siRNA-transfected cells (CM-O_{scr} or CM-O_{siArg1}, respectively) was added to mouse hepatocytes, and after 24 h, insulin signaling was analyzed. As shown in Fig. 3*C* (*left*), arginase 1 protein levels were decreased in siRNA-transfected RAW 264.7 cells compared with the scrambled condition. Importantly, insulin signaling, monitored by Akt Thr-308 phosphorylation, was markedly decreased in hepatocytes pretreated with CM-O_{siArg1} compared with those pretreated with CM-O_{scr}, although with a minor effect at the Ser-473 residue (Fig. 3*C*, *right*).

Next, we performed a broad lipidomic screening of the CM collected from RAW 264.7 cells treated with BSA, oleate, or palmitate (Fig. 4). The total amount of eicosanoids detected in the CM-P was higher compared with CM-O or control CM-B, including cyclooxygenase-derived products, such as PGE_2, PGD_2, $PGF_{2\alpha}$, tromboxane B2, 12-HHT, and 11-HETE, as well as PGD_2 dehydration metabolites like 15d-PGD_2, 15d-PGJ_2, and 15k-PGE_2. Moreover, a greater increase of lipoxygenase-derived molecular species, such as 15-HETE, prostaglandin D_2, and leucoxene B_4, was observed in CM-P as compared with CM-O. Surprisingly, levels of LTB_4 were lower in CM-O compared with those found in CM-P or CM-B.

Conditioned Medium from RAW 264.7 Macrophages Stimulated with Palmitate, but Not Oleate, Activates Stress Kinases and ER Stress Signaling and Induces Lipoapoptosis in Hepatocytes—It is well known that cytokines secreted by macrophages, such as TNFα and IL6, induce insulin resistance in hepatic cells through the activation of proinflammatory signaling pathways (37, 38). Moreover, FFAs and their metabolites have been involved in the activation of stress-mediated signaling pathways linked to chronic metabolic low grade inflammation (39). On that basis, we tested whether oleate and/or palmitate activate stress kinases in hepatocytes through their effects in macrophages. As depicted in Fig. 5*A*, the phosphorylation of

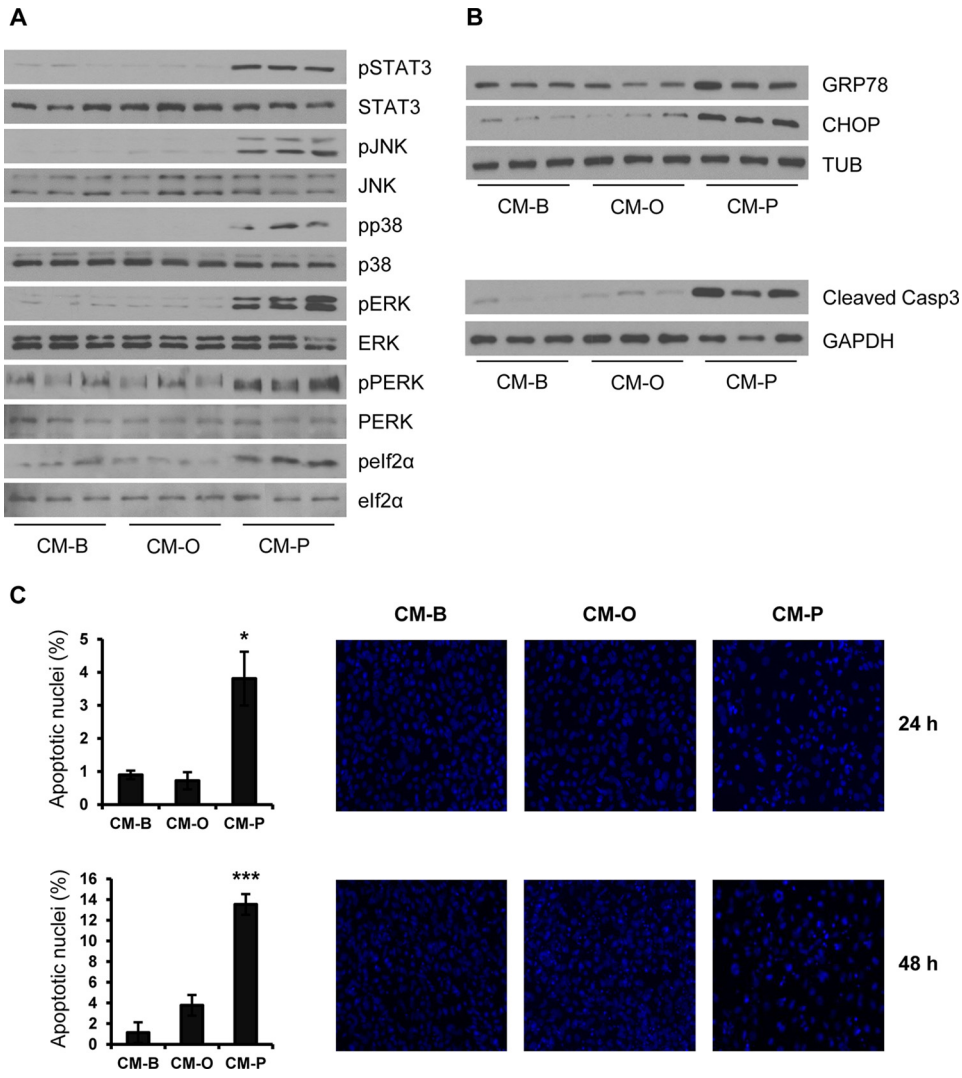

FIGURE 5. **Conditioned medium from RAW 264.7 macrophages treated with palmitate activates stress kinases and ER stress and induces lipoapoptosis in hepatocytes.** Conditioned medium from RAW 264.7 macrophages treated with BSA (*CM-B*), oleate (*CM-O*), or palmitate (*CM-P*) was added to immortalized mouse hepatocytes for several time periods (30 min (A), 24 h (*B*), and 24 and 48 h (*C*)). *A* and *B*, total protein was analyzed by Western blot using the indicated antibodies. Representative blots are shown ($n = 4$ independent experiments performed in duplicate). *C*, representative images after DAPI staining. After quantification of apoptotic nuclei from all images, results are expressed as the percentage of the number of apoptotic nuclei and are mean ± S.E. (*error bars*) ($n = 3$ independent experiments performed in duplicate). *, $p < 0.05$; ***, $p < 0.001$, CM-P *versus* CM-B.

inflammation-linked stress kinases (STAT3, JNK, p38 MAPK, and ERK) and kinases related to ER stress (PERK and eIF2α) was rapidly detected (at 30 min) in hepatocytes stimulated with CM-P but not with CM-O; the latter remained at similar basal levels of hepatic cells stimulated with CM-B. This pattern of kinase activation concurred with an increase in the expression of GRP78 and CHOP, two relevant ER stress markers, and with the detection of the active fragment of caspase-3 after 24 h of CM-P challenge (Fig. 5*B*). Conversely, neither increased GRP78 and CHOP expression nor active caspase-3 fragment were detected in hepatocytes treated with CM-O or CM-B. Notably, in hepatocytes treated with CM-P, the activation of caspase-3 correlated with increased apoptosis (Fig. 5*C*).

Conditioned Medium from Kupffer Cells Stimulated with Palmitate Activates Stress-mediated Signaling Pathways and Induces Insulin Resistance in Primary Mouse Hepatocytes—In order to confirm the differential effects of oleate and palmitate in a physiological context, we isolated and cultured Kupffer cells from C57/BL6 mice and these resident macrophages were stimulated with oleate or palmitate for 24 h. The purity of Kupper cells was checked by the analysis of CD68 and F4/80 mRNA levels (Fig. 6*A*). In agreement with the results found in RAW 264.7 cells, an increase of IL6, IL1β, TNFα, and MCP1 mRNA levels was observed only in palmitate-stimulated Kupffer cells (Fig. 6*B*). By contrast, oleate increased mRNA levels of M2 polarization markers (IL10, Mcr1, Mgl1, and arginase 1). We confirmed these data analyzing the activation of stress kinases in primary mouse hepatocytes treated with CM from Kupffer macrophages stimulated with oleate or palmitate (CMK-O or CMK-P, respectively). As a control, hepatocytes were stimulated with CM from Kupffer cells loaded with BSA (CMK-B). As shown in Fig. 6*C*, phosphorylations of STAT3, p38 MAPK, JNK, PERK, and eIF2α were observed exclusively in hepatocytes treated with CMK-P. In light of these data, CHOP and the active fragment of caspase-3, indicators of apoptosis, were detected only in hepatocytes treated with CMK-P (Fig. 6*D*).

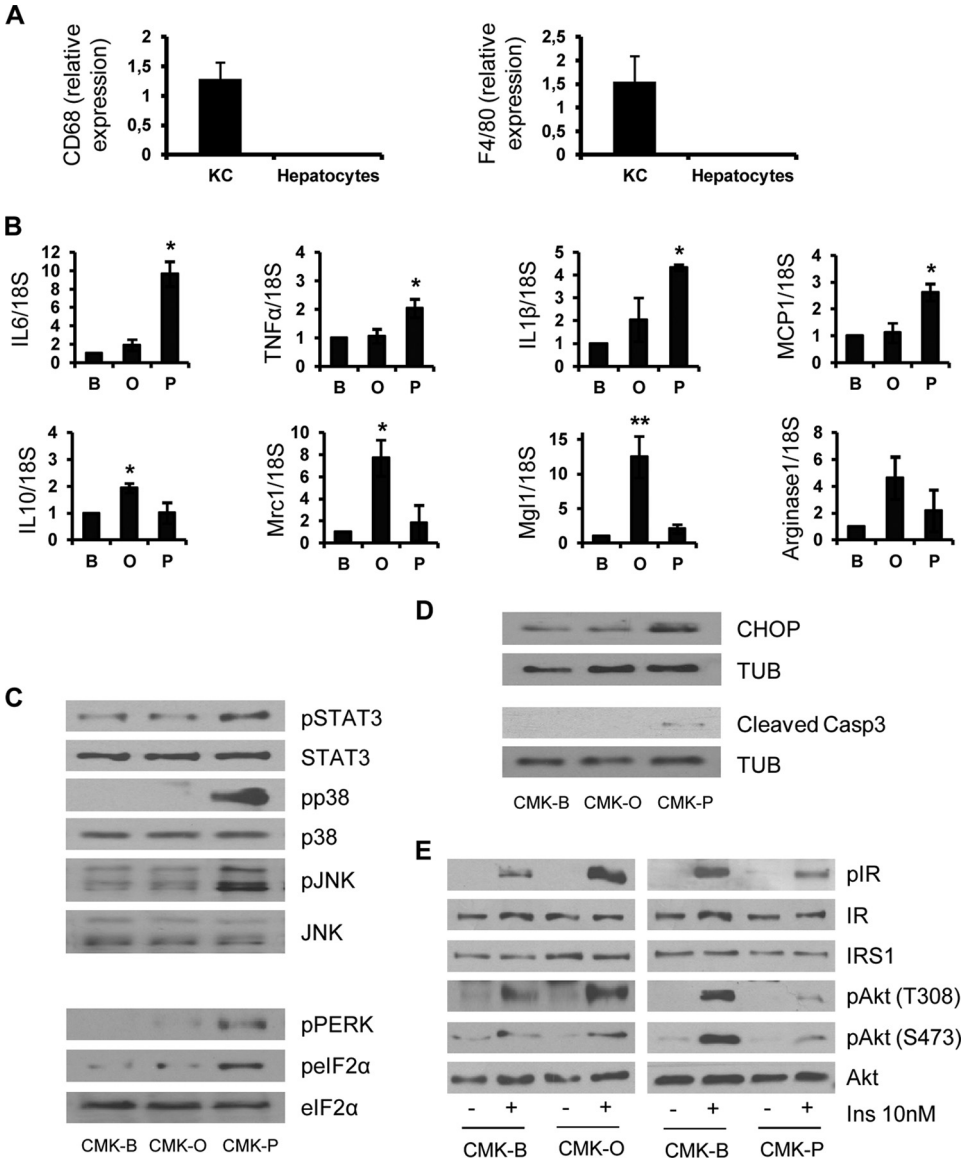

FIGURE 6. **Paracrine effects of primary Kupffer cells stimulated with palmitate or oleate in stress and insulin-mediated signaling pathways in primary mouse hepatocytes.** *A*, Kupper cells and hepatocytes were isolated from mice as described under "Experimental Procedures," and mRNA levels of CD68 and F4/80 were determined. CD68 and F4/80 were undetectable in hepatocytes ($n = 3$ independent experiments performed in duplicate). *B*, primary Kupffer cells were treated with BSA (*B*), oleate (*O*), or palmitate (*P*) for 24 h. TNFα, IL-6, IL-1β, MCP1, IL-10, arginase 1, Mcr1, and Mgl1 mRNA levels were analyzed by quantitative RT-PCR. Results are expressed as -fold increase relative to BSA condition (taken as 1) and are mean ± S.E. (*error bars*) ($n = 3$). *, $p < 0.05$; **, $p < 0.01$, *O* or *P*, respectively, *versus B*. *C* and *D*, conditioned medium from primary Kupffer cells treated with BSA (*CMK-B*), oleate (*CMK-O*), or palmitate (*CMK-P*) was added to primary mouse hepatocytes for several time periods (30 min (*C*) and 24 h (*D*)). Total protein was analyzed by Western blot using the indicated antibodies. Representative blots are shown ($n = 3$ independent experiments). *E*, CMK was added to primary hepatocytes for 24 h. Then cells were stimulated with 10 nM insulin for 10 min. Total protein was analyzed by Western blot using the indicated antibodies. Representative blots are shown ($n = 3$ independent experiments).

Next, we analyzed the effects of Kupffer cell-derived products on insulin signaling in hepatocytes. For this goal, primary hepatocytes were treated with CMK-P or CMK-O for 24 h and subsequently stimulated with 10 nM insulin for 10 min. As depicted in Fig. 6*E*, insulin-induced tyrosine phosphorylation of the IR and Akt phosphorylation at both Ser-473 and Thr-308 residues was enhanced in hepatocytes pretreated with CMK-O, whereas these responses were decreased in hepatocytes pretreated with CMK-P. These results also reflect an opposite paracrine cross-talk between hepatocytes and resident macrophages.

Lower Levels of PTP1B and LTB_4 Contribute to the Insulin Sensitization Induced by CM-O in Hepatocytes—We evaluated the possibility that changes in the expression of negative modulators of the early steps of the insulin signaling could account for the insulin sensitization induced by CM-O or CMK-O in hepatocytes. Among them, PTP1B was a potential candidate, given its ability to directly dephosphorylate tyrosine residues of the IR (40). In addition, PTEN, a lipid phosphatase, limits Akt activation by decreasing levels of phosphatidylinositol 3,4,5-triphosphate (41). Consistent with this hypothesis, we measured the expression of both phosphatases in hepatocytes incubated with CM from RAW 264.7 cells treated with BSA or oleate. As depicted in Fig. 7, *A* and *B*, PTP1B and PTEN protein content was decreased in hepatocytes treated with CM-O without changes at their mRNA levels.

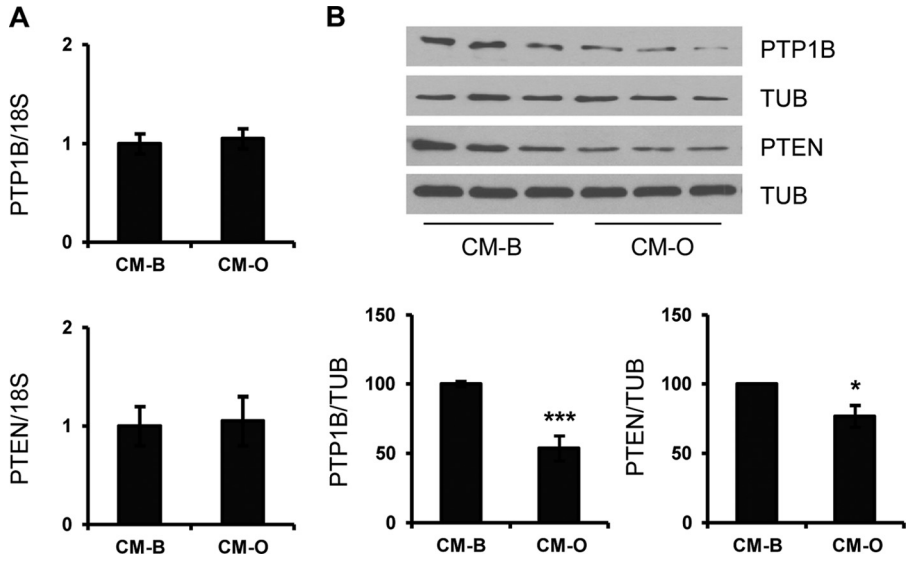

FIGURE 7. **Lower levels of PTP1B and PTEN contribute to the insulin sensitization induced by CM-O in hepatocytes.** Conditioned medium from RAW 264.7 macrophages treated with BSA (*CM-B*) or oleate (*CM-O*) was added to immortalized mouse hepatocytes for 24 h. *A*, PTP1B and PTEN mRNA levels were analyzed by quantitative RT-PCR. Results are expressed as -fold increase relative to CM-B condition (taken as 1) and are mean ± S.E. (*error bars*) ($n = 3$ independent experiments performed in duplicate). *B*, total protein was analyzed by Western blot using the indicated antibodies. Representative blots are shown. After quantification of all blots, results are expressed as the percentage of protein expression relative to CM-B condition (100%) and are mean ± S.E. ($n = 3$ independent experiments performed in duplicate). *, $p < 0.5$; ***, $p < 0.001$ CM-O *versus* CM-B.

Because we detected lower levels of LTB_4 in CM-O compared with those found in CM-P or control CM-B, we analyzed the involvement of this lipid species in the effects of oleate in insulin sensitization in hepatocytes. LTB_4 is a proinflammatory lipid mediator generated from arachidonic acid through the activities of 5,5-lipoxygenase, 5-lipoxygenase-activating protein, and leukotriene A_4 hydrolase (42, 43). First, we checked whether LTB_4 directly modulates insulin sensitivity in hepatocytes. As depicted in Fig. 8*A*, LTB_4 decreased insulin-induced IR tyrosine phosphorylation and Akt phosphorylation (Ser-473 and Thr-308) in a dose-dependent manner. These results indicate that LTB_4 *per se* induces insulin resistance in hepatocytes. Next, we evaluated whether LTB_4 was able to modulate PTP1B and PTEN expression in hepatic cells and found higher levels of both phosphatases in LTB_4-treated hepatocytes compared with the controls (Fig. 8*B*). Based on previous studies that reported on one hand increased NFκB activity in HepG2 hepatoma cells upon treatment with LTB_4 (44) and, on the other, NFκB-mediated increase in PTP1B gene expression during chronic inflammation in obesity (45), we analyzed IKK-IκBα in hepatocytes treated with LTB_4. As shown in Fig. 8*C*, LTB_4 increased IKKα/β and IκBα phosphorylation at early time periods, leading to IκBα degradation at 24 h. Notably, stress kinases that regulate insulin signaling, such as STAT3, JNK, and p38 MAPK, were also rapidly phosphorylated in response to LTB_4. As a step further, we investigated whether LTB_4 effects on PTP1B and PTEN in hepatocytes were mediated by the BLT1 receptor. For this goal, immortalized mouse hepatocytes were transfected with BLT1 or scrambled siRNA oligonucleotides. After 36 h, LTB_4 was added for a further 24 h, and PTP1B and PTEN levels were analyzed. Fig. 8*D* shows the efficacy of BLT1 silencing in immortalized hepatocytes that was able to down-regulate LTB_4-induced PTP1B and PTEN, although the latter did not reach statistical significance. Finally, hepatocytes were treated with CM-O supplemented with LTB_4 and then stimulated with insulin. As shown in Fig. 9*A*, both IR and Akt phosphorylations were decreased in hepatocytes incubated with CM-O plus LTB_4 compared with hepatocytes treated with CM-O alone. Moreover, after CM-O challenge in the presence of LTB_4, the expression of PTP1B and PTEN was increased and reached levels comparable with the CM-B condition (Fig. 9*B*). Again, this effect was particularly significant in the modulation of PTP1B levels.

DISCUSSION

In obesity-associated insulin resistance, M1-like macrophage polarization state has been associated with the enhancement of the proinflammatory milieu by the ability to secrete proinflammatory cytokines. The surrounding insulin-resistant adipocytes trigger proinflammatory signaling pathways in macrophages through their binding to Toll-like receptors (46–48). However, we know now that beyond the interplay between adipocytes and adipose tissue-resident macrophages, these inflammatory signals also dysregulate key metabolic responses in peripheral tissues, thereby exacerbating insulin resistance (3).

The liver is a target organ of the inflammatory mediators. In obesity, the hepatic lipid accumulation (first hit) together with the proinflammatory input (second hit) trigger the necroinflammatory changes that are recognized histopathologically as steatohepatitis (49). Of relevance, adipose tissue inflammation has been correlated with hepatic steatosis in humans (50). In this study, we have dissected for the first time the molecular cross-talk between signals emerging from macrophage-derived products in response to fatty acid overload and insulin signaling in hepatocytes. As a step further, we attempted to compare the responses of hepatocytes to macrophage-secreted cytokines and bioactive lipids derived from oleate or palmitate together

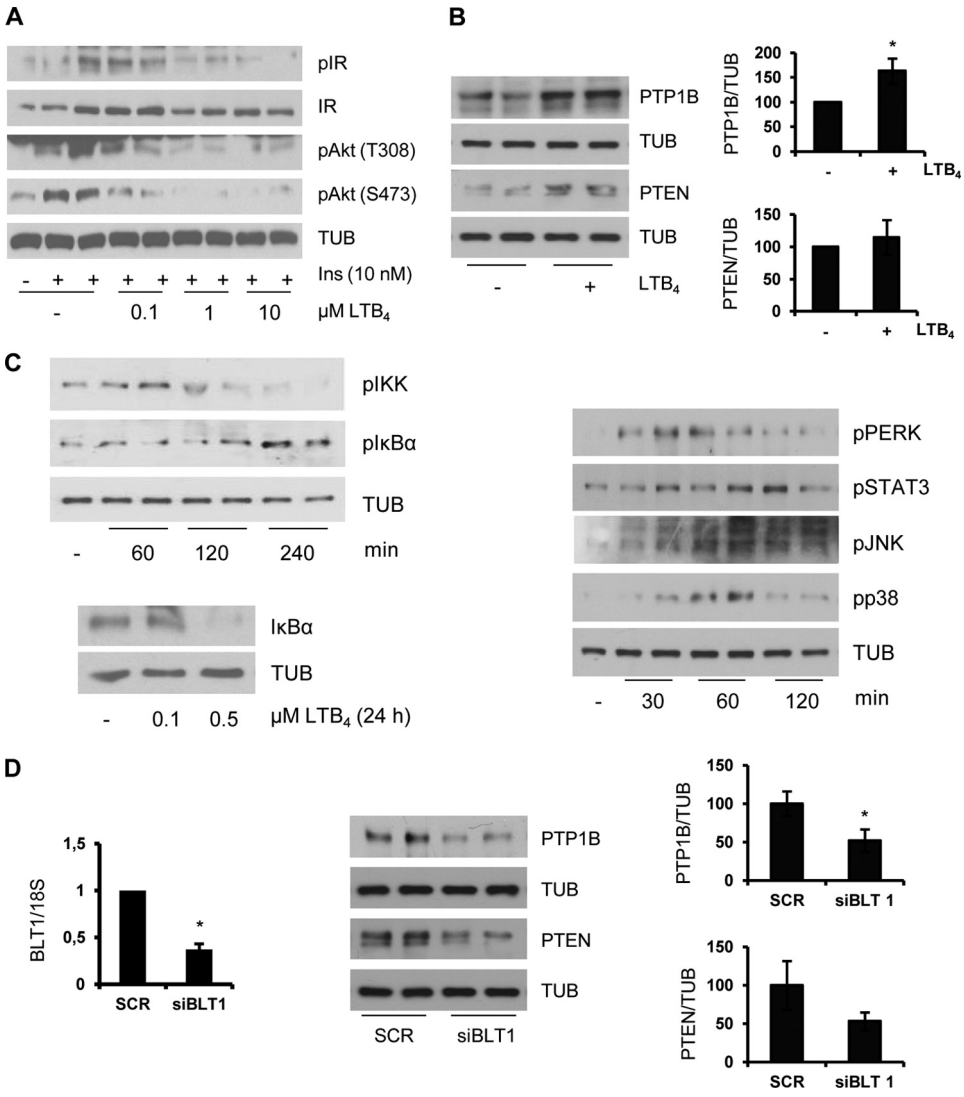

FIGURE 8. **LTB_4 inhibited insulin signaling and induced PTP1B and PTEN via BLT1 in hepatocytes.** *A*, immortalized hepatocytes were treated with various doses of LTB_4 for 24 h followed by stimulation with 10 nM insulin for 10 min. Total protein was analyzed by Western blot using the indicated antibodies. Representative blots are shown ($n = 3$ independent experiments performed in duplicate). *B*, immortalized hepatocytes were treated with 0.5 μM LTB_4 for 24 h, and the expression of PTP1B and PTEN was analyzed by Western blot. After quantification of all blots, results are expressed as the percentage of protein expression relative to control condition (100%) and are the mean ± S.E. (*error bars*) ($n = 3$ independent experiments performed in duplicate). *, $p < 0.05$ LTB_4 *versus* control. *C*, hepatocytes were treated with 0.5 μM LTB_4 for the indicated time periods, and the phosphorylation of the kinases indicated was analyzed. IκBα levels were analyzed at 24 h. Representative blots of three independent experiments are shown. *D*, hepatocytes were transfected with BLT1 or scrambled siRNA oligonucleotides, and after 36 h, cells were treated with 0.5 μM LTB_4 for 24 h. *Left*, mRNA levels of BLT1 were analyzed by RT-PCR. Results are expressed as -fold decrease relative to the scrambled condition and are mean ± S.E. ($n = 3$ independent experiments performed in duplicate). *, $p < 0.05$ BLT1 siRNA *versus* scrambled. *Right*, PTP1B and PTEN protein levels were analyzed by Western blot. After quantification of all blots, results are expressed as the percentage of protein expression relative to the scrambled condition (100%) and are mean ± S.E. ($n = 3$ independent experiments performed in duplicate). *, $p < 0.05$ BLT1 siRNA *versus* scrambled.

with FFAs mimicking the circulating proinflammatory milieu. Interestingly, an opposite response in insulin-mediated IR tyrosine phosphorylation, the earliest event in the insulin signaling cascade, was found in both mouse and human hepatocytes exposed to the CM from macrophages treated with oleate or palmitate, with a significant increase or decrease, respectively, as compared with control hepatocytes (treated with CM-BSA). This opposite response was also evidenced in Akt phosphorylation (at both Ser-473 and Thr-308), a critical node of insulin's metabolic actions in hepatic cells (51). Thus, these results suggested that oleate and palmitate induce different secretory responses in macrophages, and this might differentially modulate insulin signaling in liver cells. In light of these findings, the M1 polarization state induced by palmitate, reflected by elevated TNFα, IL6, IL1β, and inducible nitric-oxide synthase, in agreement with Samokhvalov *et al.* (30), was not observed in RAW 264.7 macrophages loaded with oleate. The absence of M1 polarization is critical to understand the modulation of insulin signaling by oleate in hepatocytes, as will be discussed below. In fact, increased arginase 1 levels reflect an M2 profile of RAW 264.7 macrophages after oleate challenge, in agreement with recent results reported by Camell and Smith (52) on the role of dietary oleic acid in M2 macrophage polarization. Indeed, when arginase 1 expression was reduced in macrophages by transfection with siRNA, the CM produced in response to oleate ($CM\text{-}O_{siArg1}$) partly reverted the enhanced

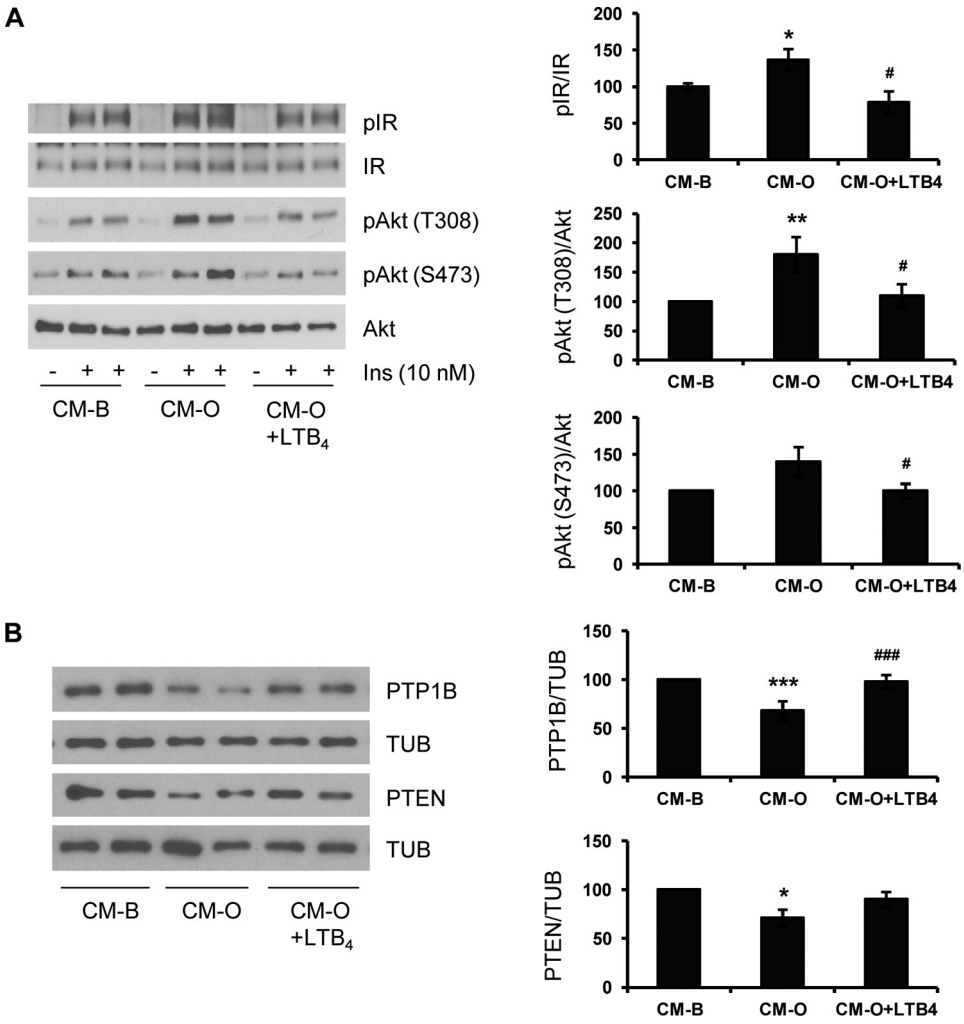

FIGURE 9. **LTB_4 impairs the enhancement of insulin signaling induced by CM-O in hepatocytes.** *A*, conditioned medium from RAW 264.7 macrophages treated with BSA (*CM-B*) or oleate (*CM-O*) was added to immortalized mouse hepatocytes for 24 h in the presence or absence of LTB_4 (0.5 μM) followed by insulin stimulation (10 nM for 10 min). Total protein was analyzed by Western blot using the indicated antibodies. Representative blots are shown ($n = 4$ independent experiments performed in duplicate). *B*, conditioned medium from RAW 264.7 macrophages treated with BSA (*CM-B*) or oleate (*CM-O*) was added to immortalized mouse hepatocytes for 24 h in the presence or absence of LTB_4 (0.5 μM). Total protein was analyzed by Western blot using the indicated antibodies. Representative blots are shown. After quantification of all blots, results are expressed as the percentage of protein expression relative to CM-B condition (100%) and are mean ± S.E. (*error bars*) ($n = 3$ independent experiments performed in duplicate). *, $p < 0.05$; **, $p < 0.01$; ***, $p < 0.001$, CM-O *versus* CM-B. #, $p < 0.05$; ###, $p < 0.001$, CM-O plus LTB_4 *versus* CM-O.

insulin signaling in hepatocytes. These results indicate that although arginase 1 is involved, a complete M2 polarization may be needed to mediate the effects of CM-O on the enhancement of insulin signaling in hepatocytes, and this approach could offer a therapeutic benefit against insulin resistance in the liver.

The ER plays a central role in the determination of cell fate under conditions of stress. Increased ER stress has been shown to contribute to the development of non-alcoholic fatty liver disease (17). In this regard, CM-P-treated hepatocytes rapidly activated the PERK branch of UPR by inducing PERK, eIF2α, and JNK phosphorylation, resulting in increased CHOP expression. Under these experimental conditions, STAT3 phosphorylation was also increased; this response is probably mediated by the proinflammatory cytokines IL6 and IL1β. Moreover, TNFα-mediating signaling might also boost JNK and p38 MAPK activation. The convergence of all of these proinflammatory signaling cascades leads to a negative cross-talk with insulin signaling, resulting in the degradation of both IR and IRS1 (Fig. 10*A*), which agrees with results reported in hepatocytes treated with palmitate (53, 54). Notably, IRS2 levels were not affected by either CM-P or CM-O in human and mouse hepatocytes, indicating that IRS2 might be more resistant to post-translational degradation compared with IRS1, as reported in primary mouse hepatocytes (55). Therefore, lower IR and IRS1 levels detected in hepatocytes stimulated with CM-P evidence the contribution of the early activation of stress kinases in the reduced insulin-mediated Akt phosphorylation. Neither the early activation of stress kinases nor CHOP expression was detected in hepatocytes treated with CM-O, highlighting the absence of oleate-mediated proinflammatory responses in the macrophage-hepatocyte axis.

Activation of Kupffer cells, the hepatic resident macrophages, to secrete proinflammatory mediators is a key event in the initiation of non-alcoholic fatty liver disease, and limiting their polarization into an M1 phenotype is considered an

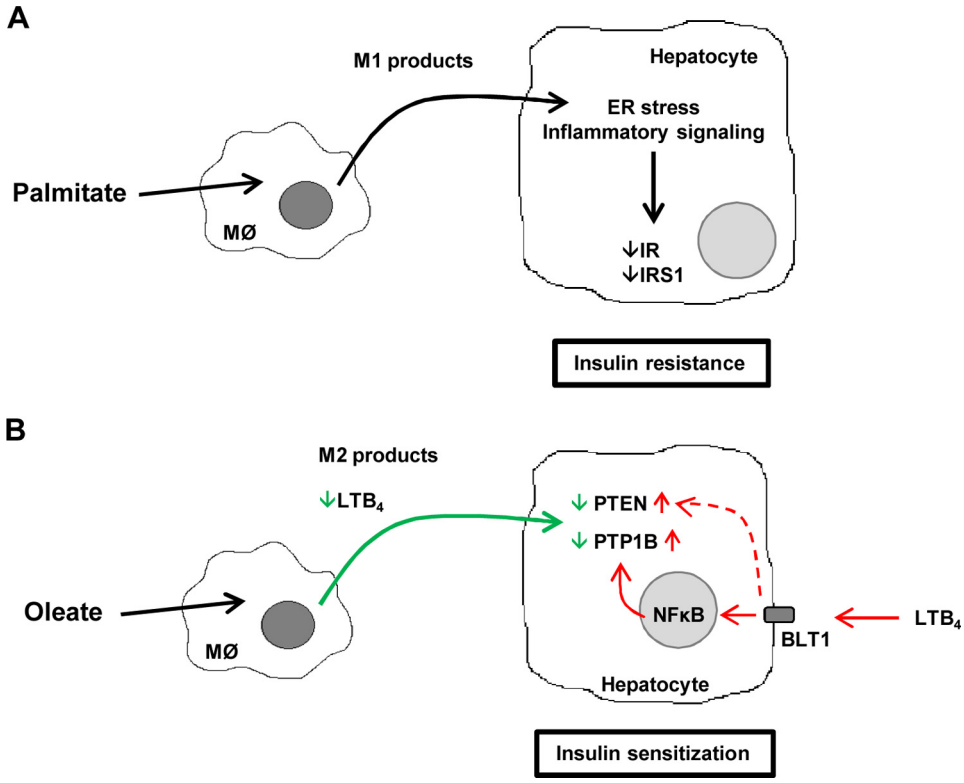

FIGURE 10. *A*, schematic representation of palmitate-induced M1 polarization of macrophages that leads to a negative cross-talk with hepatic insulin signaling through decreasing IR and IRS1. *B*, schematic representation of the beneficial effects of oleate in switching macrophage polarization by inducing M2 state to enhance insulin sensitivity in hepatocytes. The involvement of PTP1B and PTEN in the effect of LTB_4 via its receptor BLT1 is indicated.

attractive strategy against chronic liver inflammation (56–59). It has been shown that depletion of Kupffer cells using gadolinium chloride attenuated the development of steatosis and insulin resistance in the liver, suggesting an important early role for Kupffer cells in diet-induced alterations in hepatic insulin resistance (57). The differential effect of palmitate and oleate in proinflammatory cytokine secretion in RAW 264.7 macrophages was also found in primary Kupffer cells, and, importantly, similar differences were observed in the activation of stress kinases and in the modulation of insulin signaling in primary hepatocytes after CM-P challenge. Of particular relevance is the enhancement of insulin signaling in primary hepatocytes incubated with CM from Kupffer cells loaded with oleate, which reinforces the beneficial effects on insulin sensitivity in a paracrine manner.

In addition to inflammation, FFA-induced lipotoxicity contributes to the pathogenesis of non-alcoholic fatty liver disease since saturated FFAs are the more toxic lipid species (60–62). Although the evaluation of the apoptotic responses under inflammatory conditions was not the major goal of this study, we detected cleavage of caspase-3 together with an increase in the percentage of apoptotic cells in hepatocytes treated with CM-P, suggesting that the signals derived from the macrophage M1 polarization are probably involved in lipoapoptosis. This interesting issue deserves future research.

The fact that CM-O pretreatment enhanced insulin signaling in hepatocytes, reaching levels of IR and Akt phosphorylation above the controls (treated with CM-B), together with the observation that the levels of proinflammatory cytokines in CM-O did not decrease below those found in the controls prompted us to investigate additional macrophage-secreted molecules that could account for insulin sensitization. In a broad lipidomic analysis of eicosanoid species, we noted that levels of LTB_4 decreased in CM-O as compared with CM-B or CM-P. LTB_4 is involved in sustaining chronic inflammation and insulin resistance in obesity (63, 64), and more recently, deficiency of LTB_4 receptor in mice (BLT1-deficient mice) has been reported to confer protection against systemic insulin resistance and diet-induced obesity (25). Notably, the livers of BLT1-deficient mice showed decreased hepatic triglyceride accumulation and enhanced Akt phosphorylation upon insulin injection. Preincubation of mouse hepatocytes with LTB_4 decreased insulin-induced signaling at the level of the IR tyrosine phosphorylation and subsequently decreased Akt phosphorylation. Notably, in mouse hepatocytes, LTB_4 was able to up-regulate both PTP1B and PTEN, two phosphatases that negatively modulate IR and Akt, respectively (40, 41), and this effect was elicited via BLT1 because it was reverted by reducing BLT1 levels with an specific siRNA. This is the first evidence linking PTP1B and PTEN with the signaling pathways modulated by a bioactive lipid. Regarding potential signaling pathways that mediate such an effect and in agreement with previous data in HepG2 hepatoma cells (44), the NFκB pathway was activated by LTB_4 in mouse hepatocytes. Because it has been demonstrated that NFκB directly activates the transcription of the *ptpn1* gene during inflammation linked to obesity (45), our data pinpoint the NFκB-PTP1B axis as a potential mechanism by which LTB_4 negatively modulates IR tyrosine phosphoryla-

tion in hepatocytes. Based on these findings, when LTB_4 was added to CM-O insulin, sensitization was abolished in hepatocytes, as manifested by decreased IR tyrosine and Akt Ser-473 and Thr-308 phosphorylations. Importantly, the supplementation of CM-O with LTB_4 up-regulated PTP1B protein levels in hepatocytes. Previous findings have shown that macrophage-derived factors in response to LPS enhance the effect of insulin in muscle cells by increasing Akt phosphorylation, GLUT4 translocation to the plasma membrane, and glucose uptake due to an elevation of IL10 (30). Because no differences in IL10 levels were found between macrophages loaded with oleate or BSA, our data pinpoint first LTB_4 as one of the macrophage-secreted lipid species that is decreased by oleate, leading to a positive effect in the macrophage-hepatocyte axis and, second, PTP1B as a critical node of the insulin signaling that is modulated by levels of LTB_4 via NFκB. Although PTP1B has been involved in obesity and inflammation (45, 65, 66), this is the first study showing the modulation of PTP1B protein levels by a macrophage-derived lipid product from oleate because reduced levels of LTB_4 in CM-O paralleled with decreased PTP1B and enhancement of insulin-mediated IR tyrosine phosphorylation in hepatocytes. These data might be of relevance because PTP1B has emerged as a therapeutic target against obesity-mediated insulin resistance by its ability to regulate peripheral (muscle and liver) insulin sensitivity (65, 67–72) as well as the central control of appetite and energy expenditure (45, 73, 74). Besides PTP1B, CM-O decreased PTEN content, which boosts the enhancement of insulin signaling at the Akt level, and this effect was also reverted by the addition of LTB_4. Although much less is known of the regulation of PTEN expression by proinflammatory lipid mediators, our results are in line with the work of Song *et al.* (75) demonstrating that the thromboxane A2 receptor up-regulates PTEN to attenuate insulin signaling in endothelial cells. Moreover, recent data have revealed that unsaturated FFAs up-regulate microRNA-21 to induce PTEN degradation (76), strongly suggesting that the contribution of this phosphatase to the modulation of insulin signaling in hepatocytes under pro- or anti-inflammatory conditions should also be considered.

In summary, we have demonstrated an endocrine/paracrine cross-talk from macrophages/Kupffer cells to hepatocytes, which bears opposite differences, depending on the polarization state of macrophages and the factors secreted by these immune cells, as it has been manifested upon treatment with palmitate or oleate. Furthermore, LTB_4 was identified as a lipid product that mediates this cross-talk because reduced secretion of LTB_4 in oleate-stimulated macrophages concurs with the enhancement of insulin sensitivity in hepatocytes, and this effect is in part mediated by decreased PTP1B and PTEN levels. To our knowledge and as summarized in Fig. 10*B*, this is the first study providing data of the beneficial effects of oleate in switching macrophages/Kupffer polarization to increase insulin sensitization in hepatocytes.

Acknowledgment—We acknowledge J. Muntané for supplying human primary hepatocytes.

REFERENCES

1. Kahn, S. E., Hull, R. L., and Utzschneider, K. M. (2006) Mechanisms linking obesity to insulin resistance and type 2 diabetes. *Nature* **444,** 840–846
2. Attie, A. D., and Scherer, P. E. (2009) Adipocyte metabolism and obesity. *J. Lipid Res.* **50,** S395–S399
3. Lumeng, C. N., and Saltiel, A. R. (2011) Inflammatory links between obesity and metabolic disease. *J. Clin. Invest.* **121,** 2111–2117
4. Glass, C. K., and Olefsky, J. M. (2012) Inflammation and lipid signaling in the etiology of insulin resistance. *Cell Metab.* **15,** 635–645
5. Hotamisligil, G. S. (2006) Inflammation and metabolic disorders. *Nature* **444,** 860–867
6. Solinas, G., and Karin, M. (2010) JNK1 and IKKβ: molecular links between obesity and metabolic dysfunction. *FASEB J.* **24,** 2596–2611
7. Meshkani, R., and Adeli, K. (2009) Hepatic insulin resistance, metabolic syndrome and cardiovascular disease. *Clin. Biochem.* **42,** 1331–1346
8. Suchy, D., Łabuzek, K., Machnik, G., Kozłowski, M., and Okopień, B. (2013) SOCS and diabetes: ups and downs of a turbulent relationship. *Cell Biochem. Funct.* **31,** 181–195
9. Nieto-Vazquez, I., Fernández-Veledo, S., de Alvaro, C., Rondinone, C. M., Valverde, A. M., and Lorenzo, M. (2007) Protein-tyrosine phosphatase 1B-deficient myocytes show increased insulin sensitivity and protection against tumor necrosis factor-alpha-induced insulin resistance. *Diabetes* **56,** 404–413
10. Nieto-Vazquez, I., Fernández-Veledo, S., de Alvaro, C., and Lorenzo, M. (2008) Dual role of interleukin-6 in regulating insulin sensitivity in murine skeletal muscle. *Diabetes* **57,** 3211–3221
11. Roden, M., Price, T. B., Perseghin, G., Petersen, K. F., Rothman, D. L., Cline, G. W., and Shulman, G. I. (1996) Mechanism of free fatty acid-induced insulin resistance in humans. *J. Clin. Invest.* **97,** 2859–2865
12. Park, E., Wong, V., Guan, X., Oprescu, A. I., and Giacca, A. (2007) Salicylate prevents hepatic insulin resistance caused by short-term elevation of free fatty acids *in vivo*. *J. Endocrinol.* **195,** 323–331
13. Schwenger, K. J., and Allard, J. P. (2014) Clinical approaches to non-alcoholic fatty liver disease. *World J. Gastroenterol.* **20,** 1712–1723
14. Yuan, M., Konstantopoulos, N., Lee, J., Hansen, L., Li, Z. W., Karin, M., and Shoelson, S. E. (2001) Reversal of obesity- and diet-induced insulin resistance with salicylates or targeted disruption of Ikkβ. *Science* **293,** 1673–1677
15. Hirosumi, J., Tuncman, G., Chang, L., Görgün, C. Z., Uysal, K. T., Maeda, K., Karin, M., and Hotamisligil, G. S. (2002) A central role for JNK in obesity and insulin resistance. *Nature* **420,** 333–336
16. Wellen, K. E., and Hotamisligil, G. S. (2005) Inflammation, stress, and diabetes. *J. Clin. Invest.* **115,** 1111–1119
17. Ozcan, U., Cao, Q., Yilmaz, E., Lee, A. H., Iwakoshi, N. N., Ozdelen, E., Tuncman, G., Görgün, C., Glimcher, L. H., and Hotamisligil, G. S. (2004) Endoplasmic reticulum stress links obesity, insulin action, and type 2 diabetes. *Science* **306,** 457–461
18. Gregor, M. F., Yang, L., Fabbrini, E., Mohammed, B. S., Eagon, J. C., Hotamisligil, G. S., and Klein, S. (2009) Endoplasmic reticulum stress is reduced in tissues of obese subjects after weight loss. *Diabetes* **58,** 693–700
19. Scull, C. M., and Tabas, I. (2011) Mechanisms of ER stress-induced apoptosis in atherosclerosis. *Arterioscler. Thromb. Vasc. Biol.* **31,** 2792–2797
20. Ozcan, U., Yilmaz, E., Ozcan, L., Furuhashi, M., Vaillancourt, E., Smith, R. O., Görgün, C. Z., and Hotamisligil, G. S. (2006) Chemical chaperones reduce ER stress and restore glucose homeostasis in a mouse model of type 2 diabetes. *Science* **313,** 1137–1140
21. Kars, M., Yang, L., Gregor, M. F., Mohammed, B. S., Pietka, T. A., Finck, B. N., Patterson, B. W., Horton, J. D., Mittendorfer, B., Hotamisligil, G. S., and Klein, S. (2010) Tauroursodeoxycholic acid may improve liver and muscle but not adipose tissue insulin sensitivity in obese men and women. *Diabetes* **59,** 1899–1905
22. Norris, P. C., and Dennis, E. A. (2014) A lipidomic perspective on inflammatory macrophage eicosanoid signaling. *Adv. Biol. Regul.* **54,** 99–110
23. Novgorodtseva, T. P., Karaman, Y. K., Zhukova, N. V., Lobanova, E. G., Antonyuk, M. V., and Kantur, T. A. (2011) Composition of fatty acids in plasma and erythrocytes and eicosanoids level in patients with metabolic syndrome. *Lipids Health Dis.* **10,** 82

24. Henkel, J., Neuschäfer-Rube, F., Pathe-Neuschäfer-Rube, A., and Püschel, G. P. (2009) Aggravation by prostaglandin E2 of interleukin-6-dependent insulin resistance in hepatocytes. *Hepatology* **50,** 781–790
25. Spite, M., Hellmann, J., Tang, Y., Mathis, S. P., Kosuri, M., Bhatnagar, A., Jala, V. R., and Haribabu, B. (2011) Deficiency of the leukotriene B4 receptor, BLT-1, protects against systemic insulin resistance in diet-induced obesity. *J. Immunol.* **187,** 1942–1949
26. Kamei, N., Tobe, K., Suzuki, R., Ohsugi, M., Watanabe, T., Kubota, N., Ohtsuka-Kowatari, N., Kumagai, K., Sakamoto, K., Kobayashi, M., Yamauchi, T., Ueki, K., Oishi, Y., Nishimura, S., Manabe, I., Hashimoto, H., Ohnishi, Y., Ogata, H., Tokuyama, K., Tsunoda, M., Ide, T., Murakami, K., Nagai, R., and Kadowaki, T. (2006) Overexpression of monocyte chemoattractant protein-1 in adipose tissues causes macrophage recruitment and insulin resistance. *J. Biol. Chem.* **281,** 26602–26614
27. Weisberg, S. P., McCann, D., Desai, M., Rosenbaum, M., Leibel, R. L., and Ferrante, A. W., Jr. (2003) Obesity is associated with macrophage accumulation in adipose tissue. *J. Clin. Invest.* **112,** 1796–1808
28. Xu, J., Zheng, S. L., Komiya, A., Mychaleckyj, J. C., Isaacs, S. D., Chang, B., Turner, A. R., Ewing, C. M., Wiley, K. E., Hawkins, G. A., Bleecker, E. R., Walsh, P. C., Meyers, D. A., and Isaacs, W. B. (2003) Common sequence variants of the macrophage scavenger receptor 1 gene are associated with prostate cancer risk. *Am. J. Hum. Genet.* **72,** 208–212
29. Lumeng, C. N., Bodzin, J. L., and Saltiel, A. R. (2007) Obesity induces a phenotypic switch in adipose tissue macrophage polarization. *J. Clin. Invest.* **117,** 175–184
30. Samokhvalov, V., Bilan, P. J., Schertzer, J. D., Antonescu, C. N., and Klip, A. (2009) Palmitate- and lipopolysaccharide-activated macrophages evoke contrasting insulin responses in muscle cells. *Am. J. Physiol. Endocrinol Metab* **296,** E37–E46
31. Kewalramani, G., Fink, L. N., Asadi, F., and Klip, A. (2011) Palmitate-activated macrophages confer insulin resistance to muscle cells by a mechanism involving protein kinase C θ and ϵ. *PLoS One* **6,** e26947
32. Spector, A. A. (1986) Structure and lipid binding properties of serum albumin. *Methods Enzymol.* **128,** 320–339
33. Gonzalez-Rodriguez, A., Clampit, J. E., Escribano, O., Benito, M., Rondinone, C. M., and Valverde, A. M. (2007) Developmental switch from prolonged insulin action to increased insulin sensitivity in protein tyrosine phosphatase 1B-deficient hepatocytes. *Endocrinology* **148,** 594–608
34. Pichard, L., Raulet, E., Fabre, G., Ferrini, J. B., Ourlin, J. C., and Maurel, P. (2006) Human hepatocyte culture. *Methods Mol. Biol.* **320,** 283–293
35. Benveniste, R., Danoff, T. M., Ilekis, J., and Craig, H. R. (1988) Epidermal growth factor receptor numbers in male and female mouse primary hepatocyte cultures. *Cell Biochem. Funct.* **6,** 231–235
36. Dumlao, D. S., Buczynski, M. W., Norris, P. C., Harkewicz, R., and Dennis, E. A. (2011) High-throughput lipidomic analysis of fatty acid derived eicosanoids and *N*-acylethanolamines. *Biochim. Biophys. Acta* **1811,** 724–736
37. Hotamisligil, G. S., and Spiegelman, B. M. (1994) Tumor necrosis factor alpha: a key component of the obesity-diabetes link. *Diabetes* **43,** 1271–1278
38. Zhou, L., Sell, H., Eckardt, K., Yang, Z., and Eckel, J. (2007) Conditioned medium obtained from *in vitro* differentiated adipocytes and resistin induce insulin resistance in human hepatocytes. *FEBS Lett.* **581,** 4303–4308
39. Fu, S., Watkins, S. M., and Hotamisligil, G. S. (2012) The role of endoplasmic reticulum in hepatic lipid homeostasis and stress signaling. *Cell Metab.* **15,** 623–634
40. Salmeen, A., Andersen, J. N., Myers, M. P., Tonks, N. K., and Barford, D. (2000) Molecular basis for the dephosphorylation of the activation segment of the insulin receptor by protein tyrosine phosphatase 1B. *Mol. Cell* **6,** 1401–1412
41. Maehama, T., and Dixon, J. E. (1998) The tumor suppressor, PTEN/MMAC1, dephosphorylates the lipid second messenger, phosphatidylinositol 3,4,5-trisphosphate. *J. Biol. Chem.* **273,** 13375–13378
42. Samuelsson, B., Dahlén, S. E., Lindgren, J. A., Rouzer, C. A., and Serhan, C. N. (1987) Leukotrienes and lipoxins: structures, biosynthesis, and biological effects. *Science* **237,** 1171–1176
43. Haeggström, J. Z. (2004) Leukotriene A4 hydrolase/aminopeptidase, the gatekeeper of chemotactic leukotriene B4 biosynthesis. *J. Biol. Chem.* **279,** 50639–50642
44. Zhao, Y., Wang, W., Wang, Q., Zhang, X., and Ye, L. (2012) Lipid metabolism enzyme 5-LOX and its metabolite LTB4 are capable of activating transcription factor NF-κB in hepatoma cells. *Biochem. Biophys. Res. Commun.* **418,** 647–651
45. Zabolotny, J. M., Kim, Y. B., Welsh, L. A., Kershaw, E. E., Neel, B. G., and Kahn, B. B. (2008) Protein-tyrosine phosphatase 1B expression is induced by inflammation *in vivo*. *J. Biol. Chem.* **283,** 14230–14241
46. Nguyen, M. T., Satoh, H., Favelyukis, S., Babendure, J. L., Imamura, T., Sbodio, J. I., Zalevsky, J., Dahiyat, B. I., Chi, N. W., and Olefsky, J. M. (2005) JNK and tumor necrosis factor-α mediate free fatty acid-induced insulin resistance in 3T3-L1 adipocytes. *J. Biol. Chem.* **280,** 35361–35371
47. Nguyen, M. T., Favelyukis, S., Nguyen, A. K., Reichart, D., Scott, P. A., Jenn, A., Liu-Bryan, R., Glass, C. K., Neels, J. G., and Olefsky, J. M. (2007) A subpopulation of macrophages infiltrates hypertrophic adipose tissue and is activated by free fatty acids via Toll-like receptors 2 and 4 and JNK-dependent pathways. *J. Biol. Chem.* **282,** 35279–35292
48. Shi, H., Kokoeva, M. V., Inouye, K., Tzameli, I., Yin, H., and Flier, J. S. (2006) TLR4 links innate immunity and fatty acid-induced insulin resistance. *J. Clin. Invest.* **116,** 3015–3025
49. Day, C. P., and James, O. F. (1998) Steatohepatitis: a tale of two "hits"? *Gastroenterology* **114,** 842–845
50. Cancello, R., Tordjman, J., Poitou, C., Guilhem, G., Bouillot, J. L., Hugol, D., Coussieu, C., Basdevant, A., Bar Hen, A., Bedossa, P., Guerre-Millo, M., and Clément, K. (2006) Increased infiltration of macrophages in omental adipose tissue is associated with marked hepatic lesions in morbid human obesity. *Diabetes* **55,** 1554–1561
51. Taniguchi, C. M., Emanuelli, B., and Kahn, C. R. (2006) Critical nodes in signalling pathways: insights into insulin action. *Nat. Rev. Mol. Cell Biol.* **7,** 85–96
52. Camell, C., and Smith, C. W. (2013) Dietary oleic acid increases m2 macrophages in the mesenteric adipose tissue. *PLoS One* **8,** e75147
53. Ruddock, M. W., Stein, A., Landaker, E., Park, J., Cooksey, R. C., McClain, D., and Patti, M. E. (2008) Saturated fatty acids inhibit hepatic insulin action by modulating insulin receptor expression and post-receptor signalling. *J. Biochem.* **144,** 599–607
54. Lei, H., Lu, F., Dong, H., Xu, L., Wang, J., Zhao, Y., and Huang, Z. (2011) Genistein reverses free fatty acid-induced insulin resistance in HepG2 hepatocytes through targeting JNK. *J. Huazhong Univ. Sci. Technolog. Med. Sci.* **31,** 185–189
55. Leng, S., Zhang, W., Zheng, Y., Liberman, Z., Rhodes, C. J., Eldar-Finkelman, H., and Sun, X. J. (2010) Glycogen synthase kinase 3 β mediates high glucose-induced ubiquitination and proteasome degradation of insulin receptor substrate 1. *J. Endocrinol.* **206,** 171–181
56. Gao, B. (2010) Natural killer group 2 member D, its ligands, and liver disease: good or bad? *Hepatology* **51,** 8–11
57. Huang, W., Metlakunta, A., Dedousis, N., Zhang, P., Sipula, I., Dube, J. J., Scott, D. K., and O'Doherty, R. M. (2010) Depletion of liver Kupffer cells prevents the development of diet-induced hepatic steatosis and insulin resistance. *Diabetes* **59,** 347–357
58. Arkan, M. C., Hevener, A. L., Greten, F. R., Maeda, S., Li, Z. W., Long, J. M., Wynshaw-Boris, A., Poli, G., Olefsky, J., and Karin, M. (2005) IKK-β links inflammation to obesity-induced insulin resistance. *Nat. Med.* **11,** 191–198
59. Odegaard, J. I., Ricardo-Gonzalez, R. R., Red Eagle, A., Vats, D., Morel, C. R., Goforth, M. H., Subramanian, V., Mukundan, L., Ferrante, A. W., and Chawla, A. (2008) Alternative M2 activation of Kupffer cells by PPARdelta ameliorates obesity-induced insulin resistance. *Cell Metab.* **7,** 496–507
60. Malhi, H., and Gores, G. J. (2008) Molecular mechanisms of lipotoxicity in nonalcoholic fatty liver disease. *Semin. Liver Dis.* **28,** 360–369
61. Listenberger, L. L., Han, X., Lewis, S. E., Cases, S., Farese, R. V., Jr., Ory, D. S., and Schaffer, J. E. (2003) Triglyceride accumulation protects against fatty acid-induced lipotoxicity. *Proc. Natl. Acad. Sci. U.S.A.* **100,** 3077–3082
62. Mei, S., Ni, H. M., Manley, S., Bockus, A., Kassel, K. M., Luyendyk, J. P., Copple, B. L., and Ding, W. X. (2011) Differential roles of unsaturated and saturated fatty acids on autophagy and apoptosis in hepatocytes. *J. Phar-*

macol. Exp. Ther. **339,** 487–498
63. Horrillo, R., González-Périz, A., Martínez-Clemente, M., López-Parra, M., Ferré, N., Titos, E., Morán-Salvador, E., Deulofeu, R., Arroyo, V., and Clària, J. (2010) 5-Lipoxygenase activating protein signals adipose tissue inflammation and lipid dysfunction in experimental obesity. *J. Immunol.* **184,** 3978–3987
64. López-Parra, M., Titos, E., Horrillo, R., Ferré, N., González-Périz, A., Martínez-Clemente, M., Planagumà, A., Masferrer, J., Arroyo, V., and Clària, J. (2008) Regulatory effects of arachidonate 5-lipoxygenase on hepatic microsomal TG transfer protein activity and VLDL-triglyceride and apoB secretion in obese mice. *J. Lipid Res.* **49,** 2513–2523
65. González-Rodríguez, A., Más-Gutierrez, J. A., Mirasierra, M., Fernandez-Pérez, A., Lee, Y. J., Ko, H. J., Kim, J. K., Romanos, E., Carrascosa, J. M., Ros, M., Vallejo, M., Rondinone, C. M., and Valverde, A. M. (2012) Essential role of protein tyrosine phosphatase 1B in obesity-induced inflammation and peripheral insulin resistance during aging. *Aging Cell* **11,** 284–296
66. Grant, L., Shearer, K. D., Czopek, A., Lees, E. K., Owen, C., Agouni, A., Workman, J., Martin-Granados, C., Forrester, J. V., Wilson, H. M., Mody, N., and Delibegovic, M. (2014) Myeloid-cell protein tyrosine phosphatase-1B deficiency in mice protects against high-fat diet and lipopolysaccharide-induced inflammation, hyperinsulinemia, and endotoxemia through an IL-10 STAT3-dependent mechanism. *Diabetes* **63,** 456–470
67. Delibegovic, M., Bence, K. K., Mody, N., Hong, E. G., Ko, H. J., Kim, J. K., Kahn, B. B., and Neel, B. G. (2007) Improved glucose homeostasis in mice with muscle-specific deletion of protein-tyrosine phosphatase 1B. *Mol. Cell. Biol.* **27,** 7727–7734
68. Elchebly, M., Payette, P., Michaliszyn, E., Cromlish, W., Collins, S., Loy, A. L., Normandin, D., Cheng, A., Himms-Hagen, J., Chan, C. C., Ramachandran, C., Gresser, M. J., Tremblay, M. L., and Kennedy, B. P. (1999) Increased insulin sensitivity and obesity resistance in mice lacking the protein tyrosine phosphatase-1B gene. *Science* **283,** 1544–1548
69. Klaman, L. D., Boss, O., Peroni, O. D., Kim, J. K., Martino, J. L., Zabolotny, J. M., Moghal, N., Lubkin, M., Kim, Y. B., Sharpe, A. H., Stricker-Krongrad, A., Shulman, G. I., Neel, B. G., and Kahn, B. B. (2000) Increased energy expenditure, decreased adiposity, and tissue-specific insulin sensitivity in protein-tyrosine phosphatase 1B-deficient mice. *Mol. Cell. Biol.* **20,** 5479–5489
70. Delibegovic, M., Zimmer, D., Kauffman, C., Rak, K., Hong, E. G., Cho, Y. R., Kim, J. K., Kahn, B. B., Neel, B. G., and Bence, K. K. (2009) Liver-specific deletion of protein-tyrosine phosphatase 1B (PTP1B) improves metabolic syndrome and attenuates diet-induced endoplasmic reticulum stress. *Diabetes* **58,** 590–599
71. Owen, C., Lees, E. K., Grant, L., Zimmer, D. J., Mody, N., Bence, K. K., and Delibegović, M. (2013) Inducible liver-specific knockdown of protein tyrosine phosphatase 1B improves glucose and lipid homeostasis in adult mice. *Diabetologia* **56,** 2286–2296
72. González-Rodríguez, A., Mas Gutierrez, J. A., Sanz-González, S., Ros, M., Burks, D. J., and Valverde, A. M. (2010) Inhibition of PTP1B restores IRS1-mediated hepatic insulin signaling in IRS2-deficient mice. *Diabetes* **59,** 588–599
73. Bence, K. K., Delibegovic, M., Xue, B., Gorgun, C. Z., Hotamisligil, G. S., Neel, B. G., and Kahn, B. B. (2006) Neuronal PTP1B regulates body weight, adiposity and leptin action. *Nat. Med.* **12,** 917–924
74. Zabolotny, J. M., Bence-Hanulec, K. K., Stricker-Krongrad, A., Haj, F., Wang, Y., Minokoshi, Y., Kim, Y. B., Elmquist, J. K., Tartaglia, L. A., Kahn, B. B., and Neel, B. G. (2002) PTP1B regulates leptin signal transduction *in vivo*. *Dev. Cell* **2,** 489–495
75. Song, P., Zhang, M., Wang, S., Xu, J., Choi, H. C., and Zou, M. H. (2009) Thromboxane A2 receptor activates a Rho-associated kinase/LKB1/PTEN pathway to attenuate endothelium insulin signaling. *J. Biol. Chem.* **284,** 17120–17128
76. Han, S., Ritzenthaler, J. D., Zheng, Y., and Roman, J. (2008) PPARbeta/delta agonist stimulates human lung carcinoma cell growth through inhibition of PTEN expression: the involvement of PI3K and NF-κB signals. *Am. J. Physiol. Lung Cell Mol. Physiol.* **294,** L1238–L1249

Opposite Cross-Talk by Oleate and Palmitate on Insulin Signaling in Hepatocytes through Macrophage Activation

Virginia Pardo, Águeda González-Rodríguez, Carlos Guijas, Jesús Balsinde and Ángela M. Valverde

J. Biol. Chem. 2015, 290:11663-11677.
doi: 10.1074/jbc.M115.649483 originally published online March 19, 2015